ACS APPLIED MATERIALS & INTERFACES

Research Article

www.acsami.org

Highly Tunable Interfacial Adhesion of Glass Fiber by Hybrid Multilayers of Graphene Oxide and Aramid Nanofiber

Byeongho Park,[†,§] Wonoh Lee,[‡,§] Eunhee Lee,[†] Sa Hoon Min,[†] and Byeong-Su Kim*[,†]

[†]Department of Chemistry and Department of Energy Engineering, Low Dimensional Carbon Materials Center, Ulsan National Institute of Science and Technology (UNIST), Ulsan 689-798, Korea

[‡]Composites Research Center, Korea Institute of Materials Science (KIMS), 797 Changwondaero, Changwon, Gyungnam 642-831, Korea

Supporting Information

ABSTRACT: The performance of fiber-reinforced composites is governed not only by the nature of each individual component comprising the composite but also by the interfacial properties between the fiber and the matrix. We present a novel layer-by-layer (LbL) assembly for the surface modification of a glass fiber to enhance the interfacial properties between the glass fiber and the epoxy matrix. Solution-processable graphene oxide (GO) and an aramid nanofiber (ANF) were employed as active components for the LbL assembly onto the glass fiber, owing to their abundant functional groups and mechanical properties. We found that the interfacial properties of the glass fibers uniformly coated with GO and ANF multilayers, such as surface free energy and interfacial shear strength, were improved by 23.6% and 39.2%, respectively, compared with those of the bare glass fiber. In addition, the interfacial adhesion interactions between the glass fiber and the epoxy matrix were highly tunable simply by changing the composition and the architecture of layers, taking advantage of the versatility of the LbL assembly.

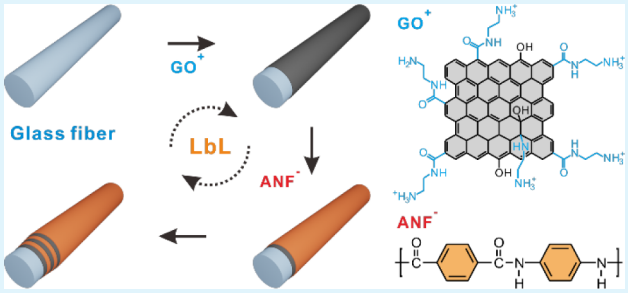

KEYWORDS: *layer-by-layer (LbL) assembly, graphene oxide, aramid nanofiber, glass fiber, interfacial shear strength*

1. INTRODUCTION

Nanocomposites containing inorganic and organic fibers within a matrix of polymers are attracting significant scientific and industrial interest in various fields with high-performance applications, including construction, transportation, sports, and aerospace.[1−3] In general, the performance of fiber-reinforced composites is governed not only by the nature of each individual component but also by the interfacial properties between the fiber and the matrix.[4] For example, the effective load transfer from the matrix to the fillers is essential to reduce stress localization and thus improves the integrated mechanical properties.[5] Consequently, significant efforts have been made toward enhancing the interfacial adhesion between the matrix and fillers in the polymer composite, such as enhancing the chemical activity of the fillers or increasing the surface area by tailoring fiber/matrix interfaces.[4,5]

Graphene, a monolayer of a two-dimensional aromatic carbon lattice, has recently emerged as a promising nanomaterial in various fields owing to its superior mechanical, thermal, and electrical properties.[6−8] In particular, solution-processable graphene oxide (GO), typically prepared by chemical exfoliation processes from graphite, possesses unique advantages suitable for nanocomposites.[9] First, abundant surface functional groups provide GO with excellent dispersity and offer opportunities for further chemical modifications with matrix polymers for interfacial engineering. Second, the unique two-dimensional sheetlike geometry of GO together with its high surface area makes it highly effective at deflecting cracks at the interface of the fiber and matrix polymer. To date, there are many reports on the production of graphene-containing polymer composites with improved static, fatigue, and electrical properties.[7,10] The successful translation of the superior material properties of graphene to macroscale composite properties often relies on the processing condition of the additive and the matrix. For example, melt blending, extrusion, postpolymerization, or in situ polymerization methods are often employed to incorporate active graphene in the polymer matrix.[11−14]

Since the development of aramid in the early 1960s, various types of aramid fiber, such as Kevlar, have received considerable attention for the design of high-performance materials, owing to their outstanding mechanical properties.[15] In particular, the ability to strengthen the matrix with high tensile strength has provided a remarkable reinforcement of polymer composites.[16,17] Recently, Kotov and co-workers reported a stable dispersion of aramid nanofiber (ANF) from Kevlar threads under a strongly basic condition, in order to overcome the issues of limited solution processability.[18] The ANF with a high

Received: November 24, 2014
Accepted: January 19, 2015
Published: January 19, 2015

DOI: 10.1021/am5082364
ACS Appl. Mater. Interfaces 2015, 7, 3329−3334

aspect ratio leads to effective stress transfer through the ANF network by reducing the stress localization at the interface between fiber filler and matrix.

We present herein a simple, alternative approach to control the interfacial interaction of a glass fiber with an epoxy matrix by coating the glass fiber with GO and ANF by using layer-by-layer (LbL) assembly (Scheme 1). As a true nanoscale blending

Scheme 1. Schematic of the Preparation of a Positively Charged Graphene Oxide (GO) and Negatively Charged Aramid Nanofiber (ANF) Multilayer Coating on a Glass Fiber via Nanoscale Blending Layer-by-Layer (LbL) Assembly

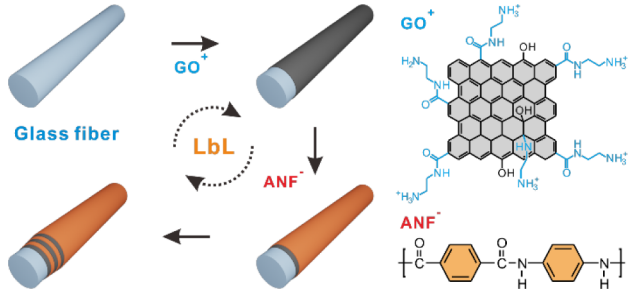

method, LbL assembly offers unique opportunities to prepare multilayer thin films of GO and ANF, with precise nanometer scale control over the thickness (i.e., the number of graphene sheets) and the structure, on solid surfaces.[19−24] There have been a number of approaches, including our own, to combine the unique properties of graphene nanosheets with the versatility of LbL assembly for electronic devices, energy storage, gas sensors, and gas barriers.[25−28] By taking advantage of LbL assembly, we also explored different combinations and sequences of layering in order to determine the impact of the architecture of coating layers on the mechanical properties of the composite. Specifically, we hypothesize that the surface functional groups present on the GO, such as epoxy groups, play an important role as potential reactive anchoring sites within the epoxy matrix. The results showed that the integration of both GO and ANF significantly improved the interfacial adhesion and mechanical properties of the composites, and most interestingly, these properties were highly tunable depending on the number and sequence of layers, as well as the composition of the multilayers at the interface of the glass fiber filler and matrix.

2. EXPERIMENTAL SECTION

Synthesis of Positively Charged Graphene Oxide (GO). Graphite oxide was synthesized by the modified Hummer's method[19,29] and then exfoliated under ultrasonication to yield a brown dispersion of GO in water. The resulting GO was negatively charged owing to the presence of chemical functional groups, such as carboxylic acids and alcohol groups. The negatively charged GO was transformed into positively charged GO by *N*-ethyl-*N*′-(3-dimethylaminopropyl)carbodiimide methiodide (EDC) chemistry. Specifically, positively charged GO was synthesized by mixing 1.88 g of EDC (Sigma-Aldrich) and 10 mL of ethylenediamine (99%, Sigma-Aldrich) in 100 mL of negatively charged GO suspension (0.5 mg/mL) and stirring for 12 h. The resulting suspension was dialyzed (MWCO 12 000−14 000, Spectra/Por) for 7 days to remove any residues and byproducts. Prior to LbL deposition, the pH of positively charged GO suspension was adjusted to 3 with the addition of 1.0 M HCl.

Synthesis of Aramid Nanofiber (ANF). ANF suspension was prepared from bulk Kevlar thread (Dupont) in dimethyl sulfoxide (DMSO) using potassium hydroxide (KOH), as previously reported by Kotov and co-workers.[18] Briefly, 0.04 g of Kevlar thread and 0.3 g of KOH were added to 100 mL of DMSO. The suspension was magnetically stirred for 1 week at room temperature, yielding a dark red ANF suspension in DMSO.

Surface Modification of Glass Fibers by LbL Assembly. The glass substrates used in the model system were cleaned using piranha solution (7:3 H_2SO_4/H_2O_2) for 1 h to remove any organic contamination. The cleaned glass substrates were treated by O_2-plasma to introduce a negatively charged surface. The substrate was first dipped in a positively charged GO solution (0.50 mg/mL) at pH 3 for 10 min. It was then rinsed in fresh deionized (DI) water for 1 min twice and then in DMSO for 2 min to remove loosely bound GO. Subsequently, the substrate was dipped in a negatively charged ANF suspension in DMSO for 10 min and washed with DMSO twice for 1 min each and DI water for 2 min, which afforded a one-bilayer film of $(GO/ANF)_1$. In the case of $(GO/PSS)_1$, the substrate was first dipped in a positively charged GO solution for 10 min, then in DI water for 1 min twice, and finally in 0.01 M NaCl for 2 min. Subsequently, the substrate was dipped in 1 wt % PSS solution [poly(sodium 4-styrenesulfonate), M_w ~70 000, Sigma-Aldrich] in 0.10 M NaCl for 10 min, after which it was washed with fresh DI water for 1 min three times each. For $(PDAC/ANF)_1$, the substrate was first dipped in 1 wt % PDAC solution [poly(diallyldimethylammonium chloride), M_w <100 000, Sigma-Aldrich], then in DI water for 1 min twice, and finally in DMSO for 2 min. Subsequently, the substrate was dipped in ANF suspension for 10 min and washed with DMSO twice for 1 min and DI water for 2 min. The above procedures were repeated to obtain the desired number of multilayers. Before surface modification of the glass fibers by LbL assembly, the glass fibers were treated with O_2-plasma for 30 s for them to obtain a negatively charged surface. Afterward, all other films were coated onto the glass fibers in a manner identical to that of the model system.

Sample Preparation for the Microbond Test. To measure the interfacial shear strength (IFSS) between the surface-modified glass fibers and the epoxy resin, microbond tests were carried out for single fibers having a microdroplet of epoxy resin.[30] Testing fibers (35 mm in length) were vertically glued to a rectangular paper frame with outer and inner dimensions of 10 × 35 and 4 × 20 mm^2 (width × length), respectively. A resin system was prepared by mixing a diglycidyl ether of bisphenol A type epoxy resin (YD128, Kukdo Chemicals) with an anhydride curing agent (KBH1089, Kukdo Chemicals) in a weight ratio of 10:9. Using the tip of a single glass fiber, a microdroplet of the prepared resin was applied to the center of the testing fiber and then cured at 120 °C for 2 h.

Characterizations. Transmission electron microscopy (TEM) characterization of the ANF solution was performed using a JEOL-2100 with an accelerating voltage of 200 kV, and the morphology of positively charged GO was investigated using tapping-mode atomic force microscopy (AFM, Nanoscope V, Veeco). The absorbance of the GO/ANF film was characterized by using UV−vis spectroscopy (Varian, Cary 5000). The surface morphology of the modified glass fibers was characterized using scanning electron microscopy (SEM, Hitachi, S-4800). The surface free energy (SFE) was characterized using a single-fiber tensiometer (K100SF, Krüss). The microbond test for measuring IFSS was performed using a dynamic mechanical analysis (DMA) machine (Q800, TA Instruments) with a film tension grip, and the sizes of the droplet were measured by an optical microscope (LV100POL, Nikon).

3. RESULTS AND DISCUSSION

Initially, GO suspensions were prepared according to the modified Hummers method with pure graphite followed by exfoliation under ultrasonication. The as-prepared suspension of GO mainly comprises single-layer graphene nanosheets having a thickness of approximately 0.70 nm with lateral dimensions of 0.70−2.0 μm, as determined by AFM (Figure

DOI: 10.1021/am5082364
ACS Appl. Mater. Interfaces 2015, 7, 3329−3334

1a). The amine functional groups were introduced on the surface of the GO through the EDC-mediated reaction between

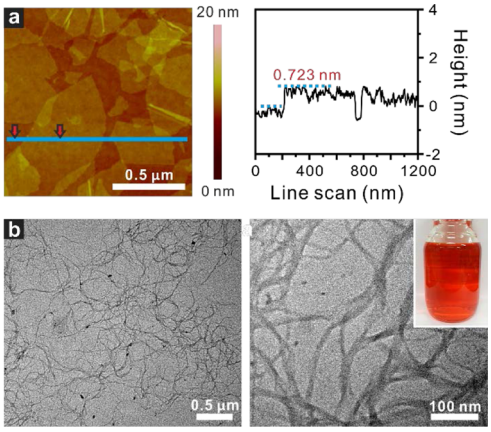

Figure 1. (a) AFM image and height profile of graphene oxide (GO) and (b) TEM images of the aramid nanofiber (ANF) derived from Kevlar threads. The inset in part b shows the suspension of the ANF in dimethyl sulfoxide.

carboxylic acids (and/or epoxides) and excess ethylenediamine ($NH_2CH_2CH_2NH_2$) to afford a positively charged GO suspension, as reported previously.[22,25,31] The as-prepared GO suspensions exhibited fairly good colloidal stability with a ζ-potential value of 38.3 mV owing to the presence of charged surface amine groups ($-NH_3^+$).

Separately, a stable dispersion of highly uniform ANFs was obtained through dissolution of commercial Kevlar fabric with KOH in DMSO based on the protocol reported by Kotov and co-workers. The diameter of the ANF was approximately 20 nm and its length was in the range of 5−10 μm, as determined from a collection of the TEM images. In addition, the abundant surface functional groups afforded the negatively charged ANF with a ζ-potential of −18.8 mV, ensuring the prerequisites for the LbL assembly with positively charged GO based on the electrostatic interactions.

With these two stable suspensions of positively charged GO and negatively charged ANFs, we fabricated multilayer films of $(GO/ANF)_n$ by alternately dip-coating onto a quartz slide as a model system to afford multilayers in an architecture of substrate/$(GO/ANF)_n$ (n = number of bilayers; typically, n = 2−10). The successful growth of $(GO/ANF)_n$ multilayers was observed from a gradual increase of the UV/vis absorbance spectra with increasing number of bilayers that shows a characteristic absorbance of GO and the ANF within the multilayer film at 222 and 330 nm, respectively (Figure 2). The linear fitting of the absorbance value at 330 nm with respect to the number of bilayers clearly demonstrates well-controlled uniform assembly of the $(GO/ANF)_n$ multilayers.

In LbL assembly, the internal structures of multilayers can be precisely tuned with a judicious choice of materials. We have exploited this principle to create another set of multilayers. First, to isolate the effects of modification from each other, we constructed only GO and ANF multilayers with conventional polyelectrolytes in a configuration of glass fiber/$(GO/PSS)_n$ and glass fiber/$(PDAC/ANF)_n$, respectively [herein, PSS is poly(styrenesulfonate) and PDAC is poly(dimethyldiallylammonium chloride)]. Second, we fabricated the two different sets of multilayers onto the glass fiber in different sequences of layering, such as glass fiber/$(GO/ANF)_n$

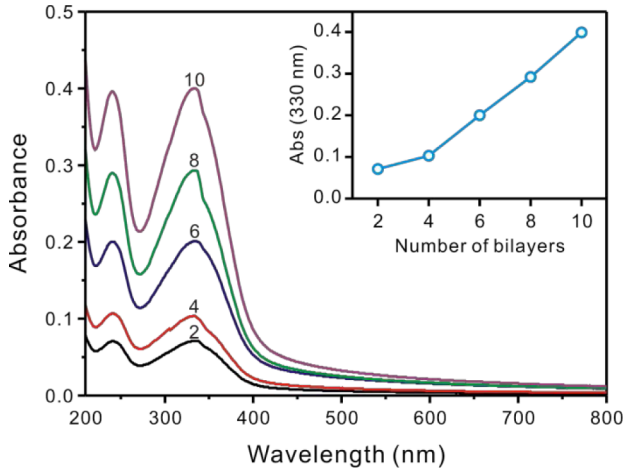

Figure 2. UV/vis spectra of GO/ANF multilayer films as a function of the number of bilayers. The inset indicates the absorbance at 330 nm depending on the number of bilayers.

and glass fiber/$(PDAC/ANF)_n/(GO/PSS)_n$. The architecture and notation of the multilayer-coated glass fibers are summarized in Table 1. As highlighted in the Introduction,

Table 1. Configuration of the Multilayer-Coated Glass Fibers

entry	architecture	notation
1	glass fiber/$(GO/PSS)_n$	GO_n
2	glass fiber/$(PDAC/ANF)_n$	ANF_n
3	glass fiber/$(GO/ANF)_n$	$(GO/ANF)_n$
4	glass fiber/$(PDAC/ANF)_n/(GO/PSS)_n$	ANF_n/GO_n

we hypothesized that the surface functional groups present on the GO and the superior mechanical property of the ANF are envisioned to provide additional opportunities to drastically improve the fiber−matrix stress transfer of glass fiber with epoxy resin for enhanced mechanical properties.

The surface morphology of the multilayers deposited on the glass fiber was examined with SEM as shown in Figure 3. It is observed that the multilayers are formed on the surface of the glass fibers with no severe agglomeration, owing to LbL assembly, which could offer fine control in the multilayer stacking. Figure 3a shows the uniformly coated morphology of GO_{10}, where GO and the polyelectrolyte are stacked. The glass fibers were well-covered by the multilayer with GO in a characteristic wrinkled surface structure, demonstrating highly flexible two-dimensional GO sheets. Likewise, ANF_{10} was successfully deposited onto the surface of the glass fibers by LbL assembly. The enlarged image in Figure 3b shows the one-dimensional fibril microstructure of the ANF in the multilayer.

For the LbL assembly between GO and ANF, parts c and d of Figure 3 show the surface morphology of $(GO/ANF)_{10}$ without the conventional polyelectrolyte and ANF_5/GO_5 with the polyelectrolyte, respectively. The multilayer of $(GO/ANF)_{10}$ provided relatively low coverage of the whole surface; in particular, some sections appear to be separated from the glass fiber. On the other hand, the coated structure of ANF_5/GO_5 is similar in morphology to that of GO_{10} that is assembled with polyelectrolyte layers. This suggests that the polyelectrolyte layers can function as a support to immobilize the microsized GO and ANF during the LbL assembly, resulting in a brick-and-mortar structure.[32] These results show that the LbL assembly makes it possible to assemble the two-dimensional

DOI: 10.1021/am5082364
ACS Appl. Mater. Interfaces 2015, 7, 3329−3334

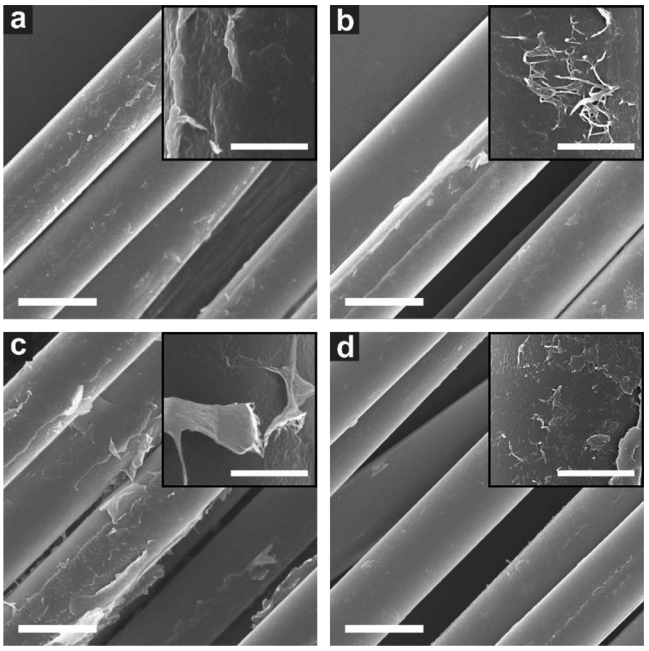

Figure 3. SEM images of multilayer-coated glass fibers of (a) GO_{10}, (b) ANF_{10}, (c) $(GO/ANF)_{10}$, and (d) ANF_5/GO_5. The inset shows an enlarged view of each glass fiber. The scale bars are 20 μm (4 μm in the insets).

GO and one-dimensional ANF within a single multilayer structure even onto the curved surface of a glass fiber. Additional cross-sectional SEM images supported the successful coating of thin layers of GO and ANF on the surface of a glass fiber (Figure S2 in Supporting Information). We also confirmed that the assembly condition did not damage the original morphology of the glass fiber during the surface modification process.

To evaluate the surface properties of multilayer-coated glass fibers, the SFE of each modified glass fiber was monitored on the basis of the Owens–Wendt method,[33] as shown in Figure 4. Specifically, the SFE of the modified glass fiber was calculated by measuring the contact angle with distilled water (H_2O) and diiodomethane (CH_2I_2) to account for the contribution of the polar and dispersive parts of the SFE, respectively. While GO_{10} had only a moderate increase of 10.4% in the dispersive part of the SFE, it showed a significant increase of 48.5% in the polar part of the SFE compared with the bare glass fiber, the SFE of which was 8.6 and 30.8 mN/m for the polar and dispersive parts, respectively. This suggests that the abundant oxygen functional groups and amine group in GO could contribute to the enhancement of the polar part of the SFE. In the case of ANF_{10}, the dispersive part of the SFE increased by 19.8% compared with that of bare glass fiber, owing to the aromatic segment and amide groups within the structure of the ANF, while the polar part decreased by 30.6%. Thus, it is considered that the ANF modification causes an increase in the dispersive part of the SFE, which is not the case for the polar part. Furthermore, the effect of the number of multilayers (i.e., multilayer thickness) was examined by utilizing the advantage of LbL assembly. Interestingly, the total SFE did not noticeably increase even in GO_{30} and ANF_{30} for the configuration of 30 bilayers (Figure S1 in Supporting Information), indicating that the LbL assembly with 10 bilayers is sufficient for the surface modification of a glass fiber.

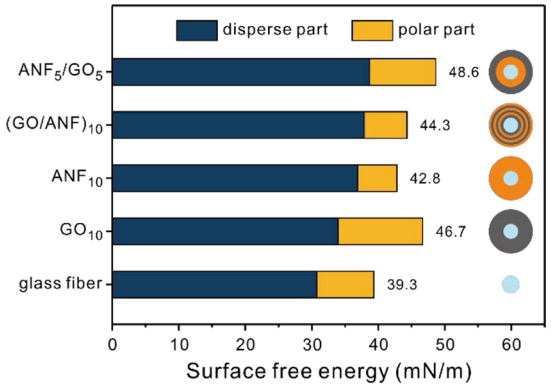

Figure 4. Surface free energy of the multilayer-coated glass fibers with different assembly and their corresponding schematics representing the glass fiber (sky blue), GO layer (gray), and ANF layer (orange).

In the hybrid architecture of GO and ANF hybrid multilayers, both $(GO/ANF)_{10}$ and ANF_5/GO_5 showed increased SFE, particularly for the dispersive part. The greatest increase in SFE was observed for the ANF_5/GO_5 configuration, where the polar and dispersive parts of the SFE were 9.93 and 38.69 mN/m, respectively. The dispersive part of the SFE of ANF_5/GO_5 exhibited a significant increase of 25.8%, whereas the polar part decreased slightly compared with that of GO_{10}, owing to the introduction of the ANF. Thus, it is obvious that the integration of GO and ANFs with LbL assembly could simultaneously improve both the polar and dispersive parts of the SFE. However, the SFE of $(GO/ANF)_{10}$ remained almost the same as that of ANF_{10}, in spite of the presence of GO layers. This suggests that the polyelectrolyte in the multilayers may play a role in the increased SFE of a glass fiber, especially for the polar part. This difference originates from the unique feature of LbL assembly that provides fine control over the architecture with a simple change in the assembly sequence.

The interfacial adhesion property between the multilayer-coated glass fibers and epoxy matrix was evaluated on the basis of IFSS using a microbond test (Figure 5a,b). The IFSS of each specimen was calculated with the equation

$$\tau_{IFSS} = \frac{F_d}{\pi D_f L_e}$$

where F_d is the pullout force at debonding, D_f is the diameter of the glass fiber, and L_e is the embedded length of the glass fiber in the epoxy matrix. In Figure 5c, the surface area of the glass fiber through the epoxy matrix and the pullout force at the debonding correlate well with a linear fit. The IFSS of all of the multilayer-coated glass fibers increased in comparison with that of a bare glass fiber, which is 20.74 MPa, in agreement with a previous report.[34,35] These enhancements in the IFSS correlate with those in the SFE of each configuration of the glass fiber, as summarized in Table 2.

As expected, ANF_5/GO_5 exhibits the greatest IFSS (39.2% greater than that of bare glass) among all the samples tested, which is consistent with the total SFE value obtained in Figure 4. Surface modification with polar functional groups leads to the enhancement of the polar part of the SFE, which can improve the degree of wetting. In addition, these functional groups participate in the curing reaction by forming covalent bonds.[36,37] Thus, the introduction of GO including abundant oxygen and amine functional groups could provide a reactive

DOI: 10.1021/am5082364
ACS Appl. Mater. Interfaces 2015, 7, 3329–3334

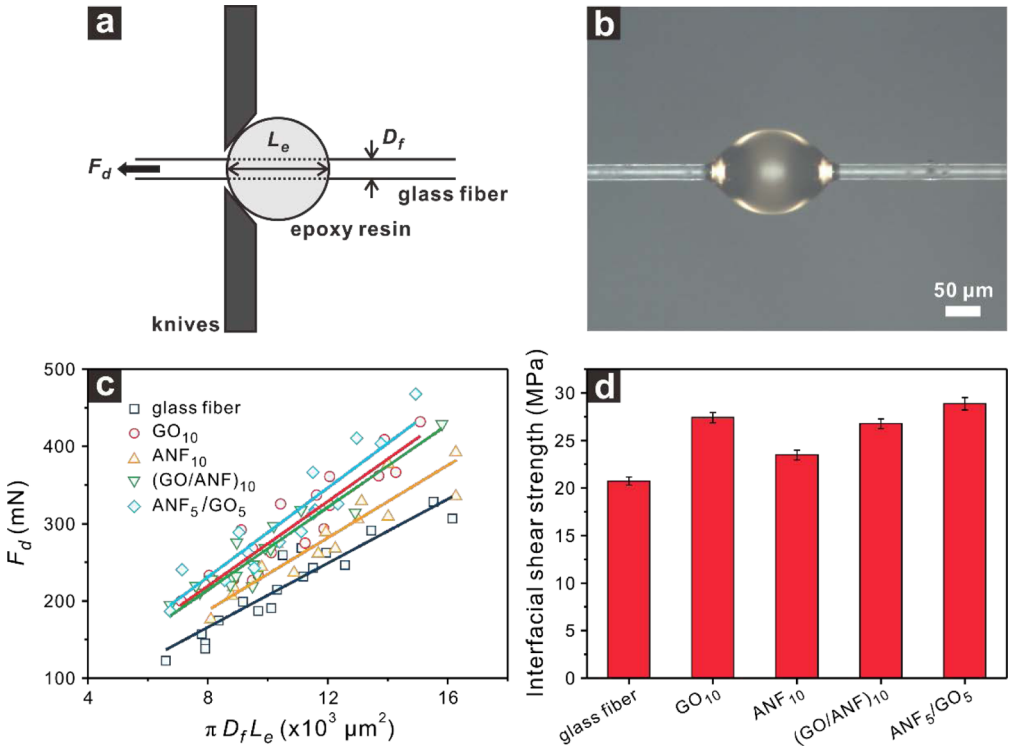

Figure 5. (a) Schematic of the microbond test for interfacial shear strength (IFSS). Epoxy resin is held in place with knives and measurement is carried out by pulling out a glass fiber. (b) Optical microscope image of the microdroplet of epoxy resin on the glass fiber. (c) Pull-out force distribution depending on the immersion area within the epoxy matrix. (d) Derived IFSS of the multilayer-coated glass fibers.

Table 2. Measured Surface Free Energy (SFE) and Interfacial Shear Strength (IFSS)

	SFE (mN/m)			
sample	polar part	dispersive part	total	IFSS (MPa)
glass fiber	8.57	30.76	39.33	20.74
GO_{10}	12.73	33.96	46.68	27.40
ANF_{10}	5.95	36.85	42.80	23.47
$(GO/ANF)_{10}$	6.45	37.86	44.31	26.77
ANF_5/GO_5	9.93	38.69	48.63	28.86

anchoring site for the epoxy matrix as well as compatibility with the epoxy matrix on the glass fiber. The introduction of the ANF significantly enhances the dispersive part of the SFE by improving the overall IFSS. Considering the SFE of $(GO/ANF)_{10}$, it is evident that the IFSS of $(GO/ANF)_{10}$ is lower than that of ANF_5/GO_5, though the number of GO and ANF layers in $(GO/ANF)_{10}$ is twice that in ANF_5/GO_5. This shows that the interfacial properties between the glass fiber and the epoxy matrix are highly tunable depending on the configuration of the GO and ANF multilayer coating, even under identical composition of multilayers.

4. CONCLUSION

In conclusion, we successfully assembled GO and ANF multilayers onto a glass fiber with facile architecture control by LbL assembly in order to enhance the interfacial properties between the glass fiber and the epoxy matrix. The LbL assembly facilitated the development of the assembly of multidimensional nanomaterials without significant phase aggregation and controlled architecture among the layers. The configuration of the GO and ANF layers had a significant influence on the surface properties of the glass fiber. In particular, the increase of polar and dispersive parts of the SFE of multilayer-coated glass fibers was mainly attributed to the GO and ANF layers, respectively. The enhancement of the IFSS between the glass fiber and epoxy matrix was consistent with that of the total SFE of the multilayer-coated glass fiber, which depends on the configuration of the GO and ANF multilayers. Therefore, the integrated architecture of GO and ANF hybrid multilayers with fine-controlled LbL assembly is expected to improve the interfacial properties of the diverse nanocomposites as well as those of the glass fiber/epoxy composites. Furthermore, it is considered that the LbL assembly could offer an opportunity to optimize the interfacial properties of nanocomposites with identical composition of coating materials.

■ ASSOCIATED CONTENT

Supporting Information

SFE of GO_{30} and ANF_{30} and cross-sectional SEM images of GO_{10}, ANF_{10}, $(GO/ANF)_{10}$, and ANF_5/GO_5. This material is available free of charge via the Internet at http://pubs.acs.org.

■ AUTHOR INFORMATION

Corresponding Author

*E-mail: bskim19@unist.ac.kr.

Author Contributions

§B.P. and W.L. contributed equally to this work.

Notes

The authors declare no competing financial interest.

■ ACKNOWLEDGMENTS

This work was supported by the Principal Research Program in the Korea Institute of Materials Science (KIMS) and by the

DOI: 10.1021/am5082364
ACS Appl. Mater. Interfaces 2015, 7, 3329−3334

National Research Foundation of Korea (NRF) grant (NRF-2014R1A2A1A11052829)

REFERENCES

(1) Benmokrane, B.; Wang, P.; Ton-That, T. M.; Rahman, H.; Robert, J. F. Durability of Glass Fiber-Reinforced Polymer Reinforcing Bars in Concrete Environment. *J. Compos. Constr.* **2002**, *6*, 143−153.

(2) Mallick, P. K. *Fiber-Reinforced Composites: Materials, Manufacturing, and Design*; Marcel Dekker: New York, 1993.

(3) De Rosa, I. M.; Sarasini, F.; Sarto, M. S.; Tamburrano, A. EMC Impact of Advanced Carbon Fiber/Carbon Nanotube Reinforced Composites for next-Generation Aerospace Applications. *IEEE Trans. Electromagn. Compat.* **2008**, *50*, 556−563.

(4) George, J.; Sreekala, M. S.; Thomas, S. A Review on Interface Modification and Characterization of Natural Fiber Reinforced Plastic Composites. *Polym. Eng. Sci.* **2001**, *41*, 1471−1485.

(5) Thostenson, E. T.; Li, W. Z.; Wang, D. Z.; Ren, Z. F.; Chou, T. W. Carbon Nanotube/Carbon Fiber Hybrid Multiscale Composites. *J. Appl. Phys.* **2002**, *91*, 6034−6037.

(6) Novoselov, K. S.; Geim, A. K.; Morozov, S. V.; Jiang, D.; Zhang, Y.; Dubonos, S. V.; Grigorieva, I. V.; Firsov, A. A. Electric Field in Atomically Thin Carbon Films. *Science* **2004**, *306*, 666−669.

(7) Stankovich, S.; Dikin, D. A.; Dommett, G. H.; Kohlhaas, K. M.; Zimney, E. J.; Stach, E. A.; Piner, R. D.; Nguyen, S. T.; Ruoff, R. S. Graphene-Based Composite Materials. *Nature* **2006**, *442*, 282−286.

(8) Schedin, F.; Geim, A. K.; Morozov, S. V.; Hill, E. W.; Blake, P.; Katsnelson, M. I.; Novoselov, K. S. Detection of Individual Gas Molecules Adsorbed on Graphene. *Nat. Mater.* **2007**, *6*, 652−655.

(9) Dreyer, D. R.; Park, S.; Bielawski, C. W.; Ruoff, R. S. The Chemistry of Graphene Oxide. *Chem. Soc. Rev.* **2010**, *39*, 228−240.

(10) Park, S.; Dikin, D. A.; Nguyen, S. T.; Ruoff, R. S. Graphene Oxide Sheets Chemically Cross-Linked by Polyallylamine. *J. Phys. Chem. C* **2009**, *113*, 15801−15804.

(11) Kim, H.; Miura, Y.; MacOsko, C. W. Graphene/Polyurethane Nanocomposites for Improved Gas Barrier and Electrical Conductivity. *Chem. Mater.* **2010**, *22*, 3441−3450.

(12) Steurer, P.; Wissert, R.; Thomann, R.; Mülhaupt, R. Functionalized Graphenes and Thermoplastic Nanocomposites Based upon Expanded Graphite Oxide. *Macromol. Rapid Commun.* **2009**, *30*, 316−327.

(13) Fang, M.; Wang, K.; Lu, H.; Yang, Y.; Nutt, S. Covalent Polymer Functionalization of Graphene Nanosheets and Mechanical Properties of Composites. *J. Mater. Chem.* **2009**, *19*, 7098−7105.

(14) Potts, J. R.; Dreyer, D. R.; Bielawski, C. W.; Ruoff, R. S. Graphene-Based Polymer Nanocomposites. *Polymer* **2011**, *52*, 5−25.

(15) Tanner, D.; Fitzgerald, J. A.; Phillips, B. R. Kevlar Story—An Advanced Materials Case Study. *Angew. Chem., Int. Ed.* **1989**, *28*, 649−654.

(16) Kitano, T.; Haghani, E.; Tanegashima, T.; Saha, P. Mechanical Properties of Glass Fiber/Organic Fiber Mixed-Mat Reinforced Thermoplastic Composites. *Polym. Compos.* **2000**, *21*, 493−505.

(17) Saikrasun, S.; Amornsakchai, T.; Sirisinha, C.; Meesiri, W.; Bualek-Limcharoen, S. Kevlar Reinforcement of Polyolefin-Based Thermoplastic Elastomer. *Polymer* **1999**, *40*, 6437−6442.

(18) Yang, M.; Cao, K.; Sui, L.; Qi, Y.; Zhu, J.; Waas, A.; Arruda, E. M.; Kieffer, J.; Thouless, M. D.; Kotov, N. A. Dispersions of Aramid Nanofibers: A New Nanoscale Building Block. *ACS Nano* **2011**, *5*, 6945−6954.

(19) Kovtyukhova, N. I. Layer-by-Layer Assembly of Ultrathin Composite Films from Micron-Sized Graphite Oxide Sheets and Polycations. *Chem. Mater.* **1999**, *11*, 771−778.

(20) Lvov, Y.; Ariga, K.; Ichinose, I.; Kunitake, T. Assembly of Multicomponent Protein Films by Means of Electrostatic Layer-by-Layer Adsorption. *J. Am. Chem. Soc.* **1995**, *117*, 6117−6123.

(21) Shen, J.; Hu, Y.; Li, C.; Qin, C.; Shi, M.; Ye, M. Layer-by-Layer Self-Assembly of Graphene Nanoplatelets. *Langmuir* **2009**, *25*, 6122−6128.

(22) Hong, J.; Han, J. Y.; Yoon, H.; Joo, P.; Lee, T.; Seo, E.; Char, K.; Kim, B.-S. Carbon-Based Layer-by-Layer Nanostructures: From Films to Hollow Capsules. *Nanoscale* **2011**, *3*, 4515−4531.

(23) Yan, Y.; Björnmalm, M.; Caruso, F. Assembly of Layer-by-Layer Particles and Their Interactions with Biological Systems. *Chem. Mater.* **2014**, *26*, 452−460.

(24) Ariga, K.; Yamauchi, Y.; Rydzek, G.; Ji, Q.; Yonamine, Y.; Kevin, C.-W.; Hill, J. P. Layer-by-Layer Nanoarchitectonics: Invention, Innovation, and Evolution. *Chem. Lett.* **2014**, *43*, 36−68.

(25) Hwang, H.; Joo, P.; Kang, M. S.; Ahn, G.; Han, J. T.; Kim, B.-S.; Cho, J. H. Highly Tunable Charge Transport in Layer-by-Layer Assembled Graphene Transistors. *ACS Nano* **2012**, *6*, 2432−2440.

(26) Yu, D.; Dai, L. Self-Assembled Graphene/Carbon Nanotube Hybrid Films for Supercapacitors. *J. Phys. Chem. Lett.* **2010**, *1*, 467−470.

(27) Ji, Q.; Honma, I.; Paek, S.-M.; Akada, M.; Hill, J. P.; Vinu, A.; Ariga, K. Layer-by-Layer Films of Graphene and Ionic Liquids for Highly Selective Gas Sensing. *Angew. Chem., Int. Ed.* **2010**, *49*, 9737−9739.

(28) Yang, Y.-H.; Bolling, L.; Priolo, M. A.; Grunlan, J. C. Super Gas Barrier and Selectivity of Graphene Oxide−Polymer Multilayer Thin Films. *Adv. Mater.* **2013**, *25*, 503−508.

(29) Hummers, W. S., Jr.; Offeman, R. E. Preparation of Graphitic Oxide. *J. Am. Chem. Soc.* **1958**, *80*, 1339.

(30) Miller, B.; Muri, P.; Rebenfeld, L. A Microbond Method for Determination of the Shear-Strength of a Fiber−Resin Interface. *Compos. Sci. Technol.* **1987**, *28*, 17−32.

(31) Lee, D. W.; Hong, T.-K.; Kang, D.; Lee, J.; Heo, M.; Kim, J. Y.; Kim, B.-S.; Shin, H. S. Highly Controllable Transparent and Conducting Thin Films Using Layer-by-Layer Assembly of Oppositely Charged Reduced Graphene Oxides. *J. Mater. Chem.* **2011**, *21*, 3438−3442.

(32) Michel, M.; Arntz, Y.; Fleith, G.; Toquant, J.; Haikel, Y.; Voegel, J.-C.; Schaaf, P.; Ball, V. Layer-by-Layer Self-Assembled Polyelectrolyte Multilayers with Embedded Liposomes: Immobilized Submicronic Reactors for Mineralization. *Langmuir* **2006**, *22*, 2358−2364.

(33) Owens, D. K.; Wendt, R. C. Estimation of the Surface Free Energy of Polymers. *J. Appl. Polym. Sci.* **1969**, *13*, 1741−1747.

(34) Netravali, A. N.; Stone, D.; Ruoff, S.; Topoleski, L. T. T. Continuous Micro-Indenter Push-Through Technique for Measuring Interfacial Shear-Strength of Fiber Composites. *Compos. Sci. Technol.* **1989**, *34*, 289−303.

(35) Moon, C. K.; Lee, J.-O.; Cho, H. H.; Kim, K. S. Effect of Diameter and Surface Treatment of Fiber on Interfacial Shear Strength in Glass Fiber/Epoxy and HDPE. *J. Appl. Polym. Sci.* **1992**, *45*, 443−450.

(36) Kang, S.; Hong, S. I.; Choe, C. R.; Park, M.; Rim, S.; Kim, J. Preparation and Characterization of Epoxy Composites Filled with Functionalized Nanosilica Particles Obtained via Sol−Gel Process. *Polymer* **2001**, *42*, 879−887.

(37) Zhu, J.; Wei, S.; Ryu, J.; Budhathoki, M.; Liang, G.; Guo, Z. In Situ Stabilized Carbon Nanofiber (CNF) Reinforced Epoxy Nanocomposites. *J. Mater. Chem.* **2010**, *20*, 4937−4948.

DOI: 10.1021/am5082364
ACS Appl. Mater. Interfaces 2015, 7, 3329−3334